Examination of Lutetium(III)-DOTA and Copper(II)-NOTA Solution Structures using EXAFS

M. Alex Brown[1], Thomas Brossard, David A. Rotsch

Argonne National Laboratory, Nuclear Engineering Division, 9700 S. Cass Ave, Lemont, IL, 60439.

Abstract

Targeted radionuclide therapy relies on the chelation of select short–lived isotopes such as ^{177}Lu and ^{67}Cu. The majority of Lu(III) and Cu(II) chelate structural information is derived from solid state diffraction data. Herein, the complexes Lu(DOTA)$^-$, Cu(NOTA)$^-$ were examined in solution using EXAFS for the first time. Both ligands were fully deprotonated and coordinated to the metal with four and three carboxylic sites for Lu(DOTA)$^-$ and Cu(NOTA)$^-$, respectively. Near-neighbor correlations from nitrogen atoms on the macrocyclic cages were also visible in the spectra in addition to the adjacent carbon backbones. Coordination numbers, bond distances, and Debye-Waller factors are reported and discussed alongside differences with known crystal structures.

Key Words: *Radionuclide therapy, lutetium, copper, DOTA, NOTA, EXAFS*

Introduction

Regarding the treatment of metastasized tumors and other pathological conditions, targeted radionuclide therapy utilizes the ionizing capabilities of relatively short-lived radioisotopes to destroy malignant biological tissues.[1] Isotopes such as ^{47}Sc, ^{67}Cu, ^{90}Y, ^{177}Lu, and ^{225}Ac emit a wide range of charged particles ideal for therapy and are being fast–tracked or have already obtained federal approval for clinical use.[2] However, a number of these isotopes exhibit valence

[1] Corresponding author: brownma@anl.gov

states – namely trivalent – in aqueous solutions that a biological system has the potential to hydrolyze and deposit in untargeted organs such as the liver and bone.[3] Chelating agents (*L*) such as *1,4,7,10-tetraazacyclododecane-1,4,7,10-tetraacetic acid* (DOTA) and *1,4,7-triazacyclononane-1,4,7-triacetic acid* (NOTA) help to maintain the solubility and biological inertness of these metals (*M*) *in vivo*.

$$M^{x+}(H_2O)_n + L^{y-} \rightarrow ML^{x-y}(H_2O)_z + (n-z)H_2O \quad (1)$$

Consequently, understanding the solution-state chelation chemistries of these complexes is important in order to design new chelate derivatives and ultimately advance clinical trials.

For most metal–chelates the accepted coordination information with respects to ionic radii, coordination numbers, bond distances and angles are derived from their crystal structures. The fact remains that in radionuclide therapy applications the complex is dissolved in aqueous solution, subject to biological *in-vivo* environments, and in the concentration ranges of *n*M to *p*M. Extended X-ray absorption fine structure (EXAFS) allows for the investigation of the solution-state structure in bulk aqueous solutions. This technique provides specific atomic neighbors, bond distances, and Debye-Waller factors that are of fundamental interest in resolving coordination information around metal ions. Furthermore, the benefits of solution EXAFS are particularly realized in the case of peptide derivatives of chelating agents where structural information is unavailable on account of difficult crystal synthesis.[4]

The generally accepted standard chelating agent for a number of metal ions – applicable in both radionuclide therapy and MRI contrasting agents DOTA.[5] The rates of lanthanide complex formation are favorable for *in-vivo* stability and driven by the enormous applications of Gd(III)-DOTA-H_2O as an MRI contrast agent the fundamental coordination chemistries and thermodynamics of $Gd(DOTA)^-$ have been resolved[6] as well as complex information with

Eu(III) and Tb(III) studied by EXAFS.[7] Other macrocyclic ligands such as *1,4,7-triazacyclononane-1,4,7-triacetic acid* (NOTA) that employ a smaller nitrogen ring cavity have found increased stability or kinetic favorability with smaller ions, such as Cu.[5 8]

This study probes the solution-state structure of the ML complexes $Lu(DOTA)^-$ and $Cu(NOTA)^-$ and compares this data to the solid-state structural data complexes in solution. Second, the intent was to compare the reported crystalline data. Finally, we report Debye-Waller information that is otherwise difficult to obtain in solution and can be correlated to the coordination environments around the hydrated or chelated metal center.

Experimental

Solutions were prepared using de-ionized (18MΩ) water. Lutetium nitrate hydrate (Sigma Aldrich, 99.9%) and copper nitrate hemipentahydrate (Sigma Aldrich, 98%) were used without further purifications. DOTA (TCI, ≥97%) and NOTA (Macrocyclics, ≥95%) were used without further purifications. Acetate buffer solutions (pH 4.7) were prepared from sodium acetate trihydrate (Sigma Aldrich). Metal chelates were prepared by dissolving excess ligand (34 mM) in 2 mL of buffer solutions containing the metal ion (5 mM) and gently mixed for one hour at approximately 90˚C. Samples were allowed to further equilibrate for another 12 hours at room temperature, filtered through a 0.2 μM syringe filter, and transferred to sample holders.

Extended x-ray absorption fine structure (EXAFS) spectra were measured on the Materials Research Collaborative Access Team (MRCAT) bending magnet beam line 10-BM at Argonne National Laboratory's Advanced Photon Source (APS).[9] The incident energy was selected using a double-crystal Si(111) monochromator with the second crystal detuned to 50% of the peak intensity. Lutetium L_3–edge and copper *K*–edge spectra were measured in

fluorescence mode using a Vortex-ME4 4-element silicon drift detector (Hitachi High-Technologies Science America, Inc.). Solutions were measured in polystyrene cuvettes with a Kapton window on one side for lower X-ray absorption and scattering from the cell walls. The cell window was oriented at a 45 degree angle with respect to the incident beam, while the detector was nominally positioned at 90 degrees with respect to the incident beam in the horizontal plane.

The background spline function was subtracted using Athena; R_{bkg} was set to 0.9 and 0.8 for Lu and Cu, respectively.[10] The wavevectors for each set of data were truncated to 2–10 A^{-1} (hanning) in order to avoid the zinc *K*–edge at 9659 eV. The *R*–range window was confined to 1–3 Å and 1.5–3.5 Å for copper and lutetium, respectively. FEFF models were generated and fit to the data using Artemis.10

Results & Discussion

a. Lutetium(III)

The coordination chemistry of the tripositive hydrated lanthanide or actinide ion in solution has appreciated the advancements in synchrotrons and has been the focus of numerous investigations.[11121314] Lutetium in dilute nitric acid was used as a reference point for the amplitude reduction factor (S_0^2) and the M–O bond length. Figure 1 shows the *R*– and *k*–space of hydrated Lu^{3+} in 0.6M nitric acid. The dominant peak represents the Lu–O interaction and the damped sine wave in *k*-space is a good indicator that only one equidistant atom neighbored the Lu center. The results are listed in Table 1. The best fit revealed eight water molecules coordinated at the same distance of 2.32 Å; textbook literature reports both eight– and nine–coordination numbers and previous studies also resolved 7.7 coordinated waters at an equal distance of 2.31Å.[1516] This coordination environment is slightly different from the hydrated Y^{3+}

ion (CN = 9.4; 2.36 Å)[17,18] but of more recent discovery are multiple hydration shells around trivalent metal ions. Skanthakumar *et al.* resolved a two-shell coordination around $Cm(H_2O)_9^{3+}$ and Lindqvist-Reis *et al.* noted a similar asymmetrical oxygen distribution for Y $(H_2O)_8^{3+}$ in solutions of iodate and perchlorate.[12,19] We refrained from forcing a second oxygen shell and truncated the fit to an eight–coordinate environment which provided a good R–factor of 2.2%. The Debye-Waller factor calculated here (0.008$Å^2$) is in good agreement with Lu EXAFS in perchloric media[16] and with trivalent *f*-block ions which generally range between 0.007 – 0.009 $Å^2$.[11]

In addition to resolving the coordination environments of Lu, we can calculate the ionic radii of the hydrated ion; a more detailed review was conducted D'Angelo *et al*.[11] Assuming the relationship

$$R_{ion} = R_{ion\text{-}H2O} - R_{H2O} \quad (2)$$

and a value of 1.35 Å for R_{H2O},[20] the resulting ionic radii is 0.97 Å which is in agreement with the reported eight-coordinate Shannon database (0.97 Å)[21] and in close agreement with the revised results (0.99 Å).[20]

The $Lu(DOTA)^-$ EXAFS data is shown in Fig. 1. To construct the FEFF models around the metal center we devised a three-shell approach – the first shell represented the coordinated carboxylates of DOTA. The second shell comprised the acyclic nitrogen donors. Third, the adjacent carbon atoms of each donor set were considered, which is now generally common practice when analyzing metal–ligand EXAFS that contains carboxylate groups.[22] The carbon atom nearest to the carboxylic site is the carbonyl atom which should reside between 3.0–3.5 Å away from the Lu centers and consequently should contribute some backscatter signal. We

applied the same rational to the nitrogen ring whose neighboring C atoms may also contribute to the spectrum.

There are three distinct features in the $Lu(DOTA)^-$ *R*–space; the data after ~3.5 Å were assumed to be insignificant contributions from multiple-scatter or noise. Both the first and second signals correlate to the Lu–O and Lu–N backscatter respectively. A good fit (*R*-factor = 0.8%) was obtained by coordinating four oxygen and nitrogen atoms from the Lu center. The inverse square relationship between the 4×Lu–O and the elongated but reduced 4×Lu–N *R*–space signal is also apparent.[23] The third signal – located at 3Å uncorrected for phase shift – correlates to the neighboring carbon atoms, specifically the carbonyls (N = 4) and the macrocyclic backbones (N = 8 or 4). The results suggest a square antriprismatic geometry; the Lu center lies closer to DOTA's four-oxygen plane than the nitrogen cage. All four carboxylates are coordinated at an equal distance of 2.29Å from the metal which is in good agreement with the crystal structure diffraction results (2.26–2.28Å).[24] The crystalline data also reports two different Lu–N bond lengths (2.59–2.64Å); we found an average scattering path of 2.59Å to be sufficient for this data set. Efforts to locate the capped water molecule (reported at ~2.4Å)[24] and to ultimately improve the fit with this extra coordination site were unsuccessful as it was rejected during the refinement. On this discussion, dehydrated metal–chelate complexes were recently reported in the case of $Cf(DTPA)^{2-}$ and $Es(DTPA)^{2-}$ when it was previously assumed that actinide(III) chelates would exhibit the hydrated species $AnDTPA(H_2O)^{2-}$.[25] Overall, structural information concerning $Lu(DOTA)^-$ in solution has by and large been derived from NMR analysis that particularly focused on conversions between isomeric forms[26] and consequently, there is very little information available for comparison in an electrolyte rich environment.

The Debye-Waller factors are listed in Table 1 and in order to decrease the number of independent variables, the first (Lu–O) and second (Lu–N + Lu–C) coordination sphere DW factors were combined. The parameter reflects the static and vibrational contributions around the metal center and is often used to describe the hydration structures of lanthanides in solution.[16] The average value for the hydrated Lu^{3+} ion (8×10^{-3}Å^2) is appreciably larger than that calculated for the oxygen pathways in $Lu(DOTA)^-$ (4×10^{-3}Å^2). Given that the temperature remained constant between the hydrated and chelated ion, we can assume the majority of the σ^2 contribution correlates to the vibrational component.[27] The differences can be ascribed to the fluctuations in coordinated neighbors about the metal center. The overall disorder and entropy is suppressed around the more kinetically-inert chelated ion relative to $Lu(H_2O)_8^{3+}$. The hydrational changes affiliated with the complexation of a lanthanide usually result in a positive entropy term (ΔS) and those changes are reflected with the lower DW factors for $Lu(DOTA)^-$.[28]

b. Copper(II)

The EXAFS of two Cu complexes are shown in Fig. 2.[29] The hydrated ion *R*–space EXAFS exhibits a prominent single peak that correlates to the Cu–O backscatter pathways. The best fit to the data revealed a (4+1) oxygen configuration located 1.96Å and 2.34Å from the metal center, respectively, with a combined DW factor of 5.5×10^{-3}Å^2. The possibility that the ion was coordinated with nitrate ligands is not unreasonable[30] since the stability constant ($\log\beta_1$) is equal to –0.01,[31] some dehydration may occur within excess nitrate solutions.[32] Previous studies on Cu–perchlorate solutions reported the hexa-aqua $Cu(H_2O)_6^{2+}$ species.[33] Nevertheless, the results presented here are in moderate agreement with literature – particularly Beagley *et al* who identified Cu–O_{eq} (1.99Å) and Cu–O_{ax} (2.29Å) by EXAFS on solutions of Cu(II)-nitrate.[34]

The spectrum of the $Cu(NOTA)^-$ complex is also shown in Fig. 2 which exhibits two prominent signals in the *R*–space. The first represents the carboxylic groups coordinated to the metal ion whereas the secondary peak located around 2.2Å (uncorrected) correlates to the nitrogen cage and auxiliary carbon backbones of the metal complex. Three oxygen atoms located at 2.0Å provided the best fit to the first peak. The second peak was fit with three Cu–N pathways but was insufficient in addressing the small tail end of the peak. The remainder was fulfilled with adjacent Cu–C pathways relating to the carboxylic groups (R = 2.9Å).

Comparing the diffraction data of $Cu(NOTA)^-$ with the EXAFS results is particularly difficult. First, solution equilibria studies revealed that all three carboxylic sites are de-protonated and coordinated to Cu^{2+} with notably high stability constants ($\log\beta_1 = 21$).[35] Yet the available solid–state crystal studies reported protonated $CuClH_2NOTA$ containing high levels of distortion in the coordination sphere on account of the counter chloride ion.[36] Further, Cu–O bond lengths vary between 1.9–2.2 Å in crystals of $CuClH_2NOTA$ and $Na[Cu(NOTA)]\cdot 2NaBr\cdot 8H_2O$.[37] The results presented here are in moderate agreement with the wide range of bond lengths but are more in line with the results of solution investigations which claim that the ligand is fully coordinated to the Cu^{2+} ion.

The Debye-Waller factor again provides us with additional coordination information between the $Cu(H_2O)_5^{2+}$ ion and the $Cu(NOTA)^-$ complex. Similar to $Lu(DOTA)^-$, a marked decrease in value is observed between the Cu–O pathway in the ion (5.5×10^{-3}Å^2) and complex (2×10^{-3}Å^2). The decrease can again be interpreted alongside the suppression in disorder and dehydration upon complexation which was previously calculated by Bevilacqua *et al* to be ΔS° = 54 $cal\cdot mol^{-1}\cdot K^{-1}$.[38]

Structural components of $Lu(DOTA)^-$ and $Cu(NOTA)^-$ chelates have been resolved by EXAFS. In the case of $Lu(DOTA)^-$, the solution complex is similar to its crystal structure with the exception of the capped water molecule, which could not be identified within this investigation. Concerning $Cu(NOTA)^-$ and its reported crystal structures, some discrepancies were observed between bond distances of Cu and nearby neighbors. As an extra contribution EXAFS also provides DW factors that reflect thermodynamic and structural information concerning atom displacements and vibrational contributions. Consequently, probing metal chelate complexes in solution by EXAFS may prove even more beneficial as new metal–chelate derivatives are synthesized for new medical isotopes.[3]

Acknowledgments

The authors would like to thank R. Jeremy Kropf (Argonne) and Mark Antonio (Argonne) for their assistance with the irradiations and interpretations of the data. This work was supported by Argonne National Laboratory under U.S. Department of Energy contract DE-AC02-06CH11357. The U.S. Government retains for itself, and others acting on its behalf, a paid-up nonexclusive, irrevocable worldwide license in said article to reproduce, prepare derivative works, distribute copies to the public, and perform publicly and display publicly, by or on behalf of the Government.

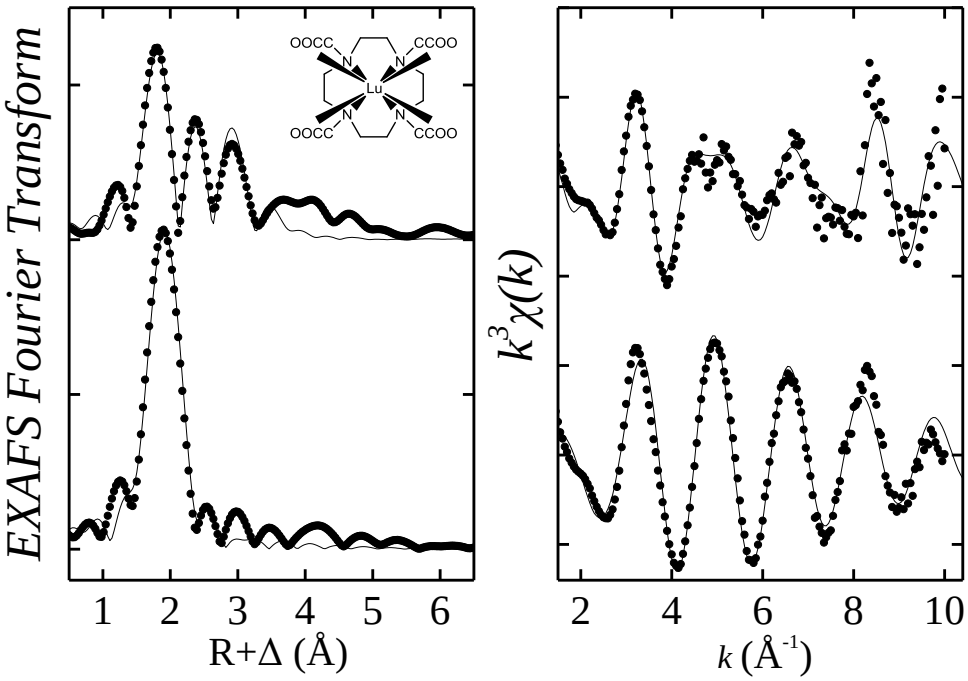

Figure 1: ***L_3–edge EXAFS of Lu(III) complexes with (top) DOTA, and (bottom) aqua ligands at room temperature. The points represent the experimental data; the solid lines represent the model fit.***

Table 1: Lutetium(III) L_3-edge EXAFS fit results. The values without uncertainties were fixed, $S_0^2 = 1.0$, and $E_0 = 9243$ eV.

	Z	CN	$\sigma^2 \times 10^{-3}$ (Å^2)	R (Å)	ΔE_0
$Lu(H_2O)_8^{3+}$	O	8 ± 1	8 ± 2	2.32 ± 0.01	6 ± 1
$Lu(DOTA)^-$	O	4	4 ± 1	2.28 ± 0.01	7.4 ± 0.8
	N	4	5 ± 2	2.59 ± 0.01	
	C_1	4	5 ± 2	3.57 ± 0.06	
	C_2	8	5 ± 2	3.40 ± 0.02	
	C_3	4	5 ± 2	3.74 ± 0.05	

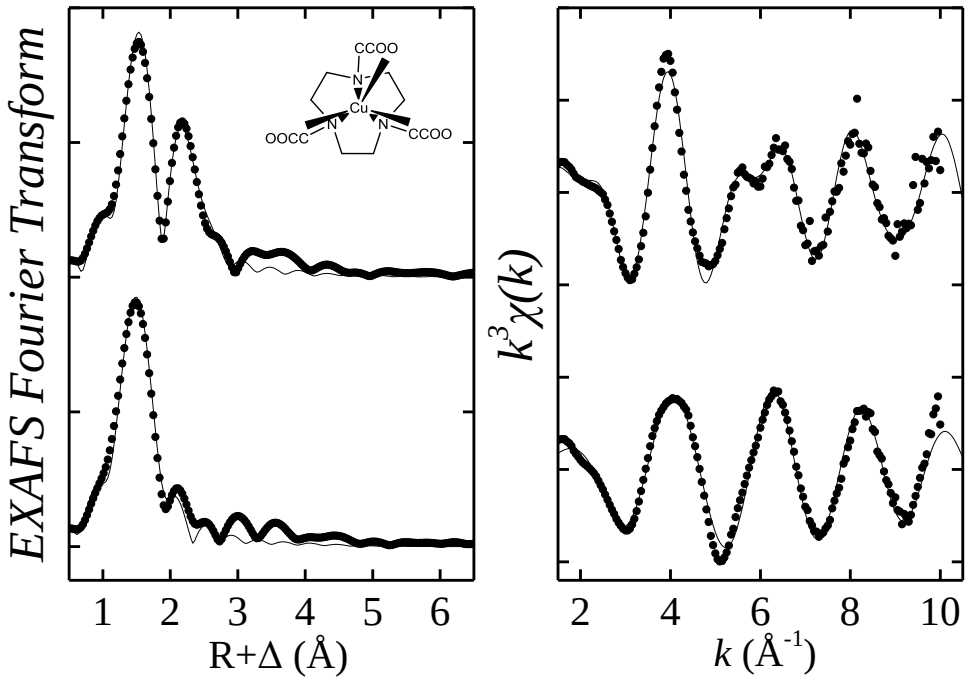

Figure 2: ***K-edge EXAFS of Cu(II) complexes with (top) NOTA and (bottom) aqua ligands at room temperature. The points represent the experimental data; the solid lines represent the model fit.***

Table 2: Copper(II) *K*-edge EXAFS fit results. The values without uncertainties were fixed, $S_0^2 = 0.9$, and $E_0 = 8991$ eV.

	Z	CN	$\sigma^2 \times 10^{-3}$ (Å^2)	R (Å)	ΔE_0
$Cu(H_2O)_5^{2+}$	O_1	4	5.5 ± 0.8	1.949 ± 0.009	-3.5 ± 0.9
	O_2	1	5.5 ± 0.8	2.34 ± 0.03	
$Cu(NOTA)^-$	O	3	2 ± 1	2.01 ± 0.01	1.8 ± 0.7
	N	3	8 ± 2	2.29 ± 0.01	
	C	7	8 ± 2	2.90 ± 0.01	

References

[1] M.R. Zalutsky, *Radionuclide Therapy* in *Radiochemistry and Radiopharmaceutical Chemistry in Life Sciences*, A. Vertes, S. Nagy, Z. Klencsar, Kluwer Academic Publishers, **2003**, pg. 315, 333.
[2] S.C. Srivastava, *Sem. Nucl. Med.* (2012) 151-163.
[3] K.A. Deal, I.A. Davis, S. Mirzadeh, S.J. Kennel, M.W. Brechbiel, *J. Med. Chem.* 42 (1999) 21988-2992.
[4] J. V. Deshmukh, G. Voll, A. Kuhlewein, H. Macke, J. Schmitt, H. Kessler, G. Gemmecker, *J. Med. Chem.* 48 (2005) 1506-1514.
[5] E.W. Price, C. Orvig, *Chem. Soc. Rev.* 43 (2014) 260-290.
[6] J. Moreau, E. Guillon, J.C. Pierrard, J Rimbault, M. Port, M. Aplincourt, *Chem. Eur. J.* 10 (2004) 5218-5232.
[7] S. Benazeth, J. Purans, M.C. Chalbot, M.K. Nguyen-van-Duong, L. Nicolas, F. Keller, A. Gaudemer, *Inorg. Chem.* 37 (1998) 3667-3674.
[8] Y. Zhang, H. Hong, J.W. Engle, J. Bean, Y. Yang, B.R. Leigh, T.E. Barnhart, W. Cai, *PLoS One* 6 (2011) e28005.
[9] C.U. Segre, N.E. Leyarovska, L.D. Chapman, W.M. Lavender, P.W. Plag, A.S. King, A.J. Kropf, B.A. Bunker, K.M. Kemner, P. Dutta, R.S. Duran, J. Kaduk, The MRCAT insertion device beamline at the Advanced Photon Source, AIP Conference Proceedings 521 (2000) 419-422.
[10] B. Ravel, M. Newville, ATHENA, ARTEMIS, HEPHAESTUS: Data Analysis for X-ray Absorption Spectroscopy Using IFEFFIT., J. Synch. Rad. 12 (2005) 537-541.
[11] P. D'Angelo, F. Martelli, R. Spezia, A. Filipponi, M.A. Denecke, *Inorg. Chem.* 52 (2013) 10318-10324.
[12] S. Skanthakumar, M.R. Antonio, R.E. Wilson, L. Soderholm, *Inorg. Chem.* 46 (2007) 3485-3491.
[13] M.P. Jensen, A.H. Bond, *J. Am. Chem. Soc.* 124 (2002) 9870-9877.
[14] M.G. Ferrier, B.W. Stein, E.R. Batista, J.M. Berg, E.R. Birnbaum, J.W. Engle, K.D. John, S.A. Kozimor, J.S. Lezama Pacheco, L.N. Redman, *ACS Cent. Sci.* 3 (2017) 176-185.
[15] S. Cotton, *Lanthanide and Actinide Chemistry*, John Wiley & Sons, Ltd., U.K. (2006) 114.
[16] T. Yamaguchi, M. Nomura, H. Wakita, J. Ohtaki, *J. Phys. Chem.* 89 (1988) 5153-5159.
[17] W.W. Rudolph, G. Irmer, *Dalton Trans.* 44 (2015) 18492.
[18] K.V. Ragnarsdottir, E.H. Oelkers, D.M. Sherman, C.R. Collins, *Chem. Geol*, 151 (1998) 29-39.
[19] P. Lindqvist-Reis, K. Lamble, S. Pattanaik, I. Persson, M. Sandström, *J. Phys. Chem. B* 104 (2000) 402-408.
[20] P. D'Angelo, A. Zitolo, V. Migliorati, G. Chillemi, M. Duvail, P. Vitorge, S. Abadie, R. Spezia, *Inorg. Chem.* 50 (2011) 4572-4579.
[21] R.D. Shannon, *Acta Crystallogr. A* 32 (1976) 751-767.
[22] M. Antonio, L. Soderhold, *X-ray absorption spectroscopy of the actinides* in *The Chemistry of the Actinides, and Transactinide Elements*, 3rd ed., Springer 5 (2006) 3138.
[23] B. Teo, *EXAFS: Basic Principles and Data Analysis*, Springer Verlag, NY (1986) 45.
[24] N. Viola-Villegas, R. P. Doyle, *Coordination Chemistry Reviews* 253 (2009) 1906-1925.
[25] G. J-P. Deblonde, M.P. Kelley, J. Su, E.R. Batista, P. Yang, C.H. Booth, R.J. Abergel, Angew. Chem. Int. Ed. 10.1002/anie.201709183
[26] S. Aime, A. Barge, M. Botta, M. Fasano, J.D. Ayala, G. Bombieri, *Inorganica Chimica Acta* 246 (1996) 423-429.
[27] T.K. Sham, J.B. Hastings, M.L. Perlman, *J. Am. Chem. Soc*. 102 (1980) 5904-5906.
[28] G.R. Choppin, *J. Less-Common Met.* 93 (1983) 323-330.
[29] J. Sheals, P, Persson, B, Hedmon, Inorg Chem. 40 (2001) 4302-4309.
[30] P.S. Salmon, G.W. Neilson, *J. Phys.: Condens. Matter* 1 (1989) 5291-5295.
[31] S. Cotton, *Lanthanide and Actinide Chemistry*, John Wiley & Sons, U.K. (2006) 36.
[32] A. Pasquarello, I. Petri, P.S. Salmon, O. Parisel, R. Car, E. Toth, D.H. Powel, H.E. Fischer, L. Helm, A.E. Merbach, *Science* 291 (2001) 856-859.
[33] T.K. Sham, J.B. Hastings, M.L. Perlman, *Chemical Physics Letters* 83 (1981) 391-396.
[34] B. Beagley, A. Eriksson, J. Lindgren, I. Persson, L.G.M. Pettersson, M. Sandstrom, U. Wahlgren, E.W. White, *J. Phys.: Condens. Matter* 1 (1989) 2395-2408.
[35] A. Bevilacqua, R.I. Gelb, W. B. Hebard, L.J. Zompa, *Inorg, Chem.* 26 (1986) 2699-2706.
[36] M.J. Van der Merwe, J.C.A Boeyens, R.D. Hancock, *Inorg. Chem.* 24 (1985) 1208.
[37] K. Weighardt, U. Bossek, P. Chaudhrui, W. Herrmann, B.C. Menke, J. Weiss, *Inorg. Chem.* 21 (1982) 4308.
[38] A. Bevilacqua, R.I. Gelb, W.B. Hebard, L.J. Zompa, *Inorg. Chem.* 26 (1986) 2699.